

Evaluation of Image Analysis Tools for Characterization of Sweet Bread Crumb Structure

Reynold R. Farrera-Rebollo · Ma. de la Paz Salgado-Cruz · Jorge Chanona-Pérez · Gustavo F. Gutiérrez-López · Liliana Alamilla-Beltrán · Georgina Calderón-Domínguez

Received: 10 June 2009 / Accepted: 5 January 2011 / Published online: 20 January 2011
© Springer Science+Business Media, LLC 2011

Abstract Many approaches to evaluate bread crumb features by applying free or at least not too expensive image analysis (IA) software have been published; however, the described procedures showed noticeable differences. The aim of this work was to compare different image scanning resolutions and thresholding techniques to quantify sweet bread crumb features (cell density, mean cell area, shape factor) and their relation with fractal dimension. Two sets of experiments were carried out, one to determine the effect of scanning resolution and thresholding method and the other to validate the previous results by evaluating breads with different crumb structures. Nine different scanning resolutions (75, 100, 150, 200, 300, 355, 435, 515, 555 dpi) and two segmentation procedures (Otsu and Manual) were tested. Three different types of commercial sweet breads and a yeasted sweet bread added with different concentrations (six, 12%) of Chia flour (*Salvia hispanica*) were evaluated. Results showed that the percentage of particles with areas between 0.1 and 4.0 mm² remained almost constant when using 350 dpi or larger resolution values, while the smallest particles (<0.1 mm²) increased their proportion up to 87% at the highest scanning resolution for both thresholding methods. IA was useful to detect crumb structure differences among commercial breads and breads added with Chia flour as obtained from cell

density (154 ± 4.6 – 246 ± 2.5) and mean cell area (0.81 ± 0.02 – 0.7 ± 0.03) results. However, the number of selected objects to calculate these parameters produced different results. The addition of 6% of Chia flour did not affect the bread crumb features, while at the largest proportion more and smaller pores were obtained. Fractal texture was useful to evaluate bread crumb structure, as it not depends on the number of particles detected.

Keywords Image analysis · Sweet bread · Crumb structure · Fractal dimension of texture

Introduction

Structure of bread crumb has been traditionally analyzed based on the experience of baker who evaluates compactness and uniformity of the bread grain, as visually perceived traits dealing with the size, shape, uniformity and wall thickness of crumb cells or pores (Rogers et al. 1995; Pylar 1988) all of them representing, at a macroscopic level, the solid and fluid phases of bread crumb (Scanlon and Aghal 2001). The fluid phase also named as cells or pores (Fig. 1) can be divided in three groups: closed, blind and flow-through pores or cells, covering diameters of a few microns to several thousand microns (Datta et al. 2007).

In recent years, image analysis (IA) has been used as quantitative tool for the assessment of crumb features (Zayas 1993; Sapirstein et al. 1994; Crowley et al. 2000; Riva and Liviero 2000; Lagrain et al. 2006; Gonzales-Barron and Butler 2006; Calderón-Domínguez et al. 2008; Ribotta et al. 2010) and digital scanners to capture bread crumb two dimensions (2D) high-resolution images (Esteller and Lannes 2008; Datta et al. 2007; Lassoued et al. 2007;

This research was financed by projects 20071179, 20080517 from the Instituto Politécnico Nacional (IPN, Mexico), and 84287, 59730 from Consejo Nacional de Ciencia y Tecnología (CONACYT-México).

R. R. Farrera-Rebollo · M. Salgado-Cruz · J. Chanona-Pérez · G. F. Gutiérrez-López · L. Alamilla-Beltrán · G. Calderón-Domínguez (✉)
Departamento de Ingeniería Bioquímica, Escuela Nacional de Ciencias Biológicas, Instituto Politécnico Nacional, Prolongación de Carpio y Plan de Ayala. Casco de Sto. Tomás, México D.F. CP. 11340, México
e-mail: gcalderon@ipn.mx

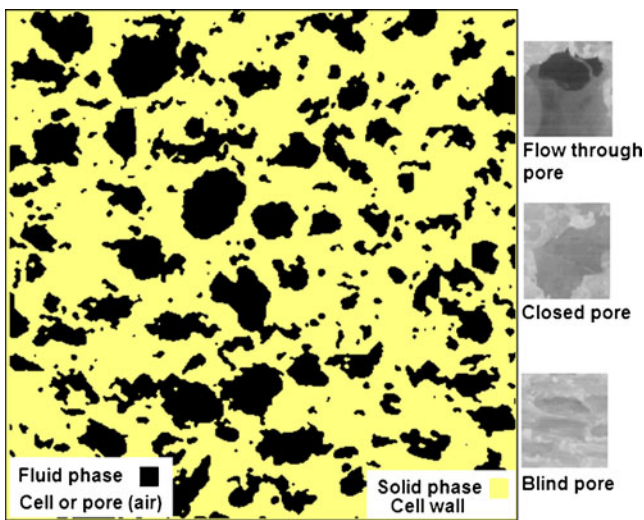


Fig. 1 Schematic diagram of the structure of bread crumb structure

Esteller et al. 2006). Hatcher et al. (2004) reported that the use of a scanner for image acquisition, for the assessment of oriental noodle appearance and colour, offers all the advantages of previously investigated camera based systems, while Esteller et al. (2006) explained that the acquisition of 2D images by flatbed scanning is fast, easy to use, economical, robust, independent of the external light conditions and with good accuracy.

In bread-making practice, IA has been used for quantifying crumb features such as cell size, cell size distribution, number of cells per unit area, cell wall thickness, void fraction and shape factor (Calderón-Domínguez et al. 2008; Rosales-Juárez et al. 2008; Gonzales-Barron and Butler 2006; Lagrain et al. 2006; Takano et al. 2002) or even the volume of the product (Chevallier et al. 2010). However, there is not yet a standardized technique for this evaluation as differences among the reported IA methodologies for acquiring images by scanning or when pre-processing or processing these images to obtain crumb features are found. Some of these differences among the reported methodologies are about the scanning resolution, where it is possible to find reports using 150 dpi (Skendi et al. 2010; Crowley et al. 2000), 200 dpi (Esteller and Lannes 2008; Esteller et al. 2006; Collar et al. 2005), 300 dpi (Pérez-Nieto et al. 2010; Lagrain et al. 2006, 2008), 350 dpi (Rosell and Santos 2010; Gonzales-Barron and Butler 2006), 550 dpi (López-Guel et al. 2010), 600 dpi (Baiano et al. 2009) or even without reporting the scanning resolution applied to the analysis. In the same context, the range of cells used to evaluate the crumb features, with some exceptions (Pérez-Nieto et al. 2010; Skendi et al. 2010; Gonzales-Barron and Butler 2008b; Crowley et al. 2000) is not mentioned. These differences in methodologies could result in different data for similar breads, making difficult to compare information among published reports.

Another parameter obtained by IA is the fractal dimension (FD) which provides a numerical descriptor of the morphology of objects with complex and irregular structures and it has been used to explain changes in the structure of food materials during or as a consequence of processing (Kerdpi boon and Devahastin 2007; Chanona et al. 2003; Rahman 1997; Barletta and Barbosa 1993; Peleg and Normand 1985). This parameter, very often a non-integer, measures the degree of irregularity of an object over multiple scales and determines how a fractal differs from Euclidean objects such as a point (FD = 0), a line (FD = 1.0), a surface (FD = 2) or a solid (FD = 3), resulting in a measure of their geometrical complexity. So a porous material, like bread, is described as a wrinkled surface that resembles a solid, with a fractal dimension between 2 and 3. Theiler (1990) cited that fractals are crinkly objects that defy conventional measures, such as length and area, and they are most often characterized by their FD, while Barret and Peleg (1995) explain that many foods, including bread, like other natural materials, are irregular in conformation and with complex geometry and structural irregularities such as pores, protuberances and apparently replicating structures and can be described in terms of their fractal dimension, which may serve as an index of morphological roughness or tortuosity.

Bread crumb features have also been characterized by fractal texture analysis (Pedreschi et al. 2000; Gonzales-Barron and Butler 2008b) where the bread grain fineness has shown good correlation with fractal dimension ($R^2 = 0.822$) when applying the relative differential box counting method, whereas grain homogeneity has been related to the mass fractal dimension ($R^2 = 0.820$) (Gonzalez-Barron and Butler 2008a). In other work, Pérez-Nieto et al. (2010) showed that fractal dimension of texture was a useful indicator of coalescence as well as to distinguish the baking time needed for crumb features to remain invariable. However, there is not reported information of fractal dimension analysis applied to sweet breads which have different crumb structure as compared to white or French breads.

A broad variety of sweet breads with different crumb characteristics can be produced. These types of breads (danish, puff pastry, pound cakes, cookies), along with white bread, are widely consumed (32 Kg annual per capita consumption) as part of daily meals in Mexico (Hernández et al. 2003).

Sweet bread quality depends on the wheat flour characteristics, on the ingredients used, as well as on the processing conditions applied, resulting in large differences in bread features among bakeries. Moreover, the use of flours other than wheat in bread making is known to change bread crumb structure and this effect has been barely studied on sweet bread. On the other hand, it is a common practice that bakers evaluate, based on their own experience, the effect of adding new ingredients or additives on

bread crumb characteristics, as they do not have simple quantitative methods to analyze them, for which a low-cost IA methodology to evaluate bread crumb structure or to help standardizing bread quality would be useful. The aim of this work was to compare different image scanning resolutions and thresholding techniques and to quantify the differences in crumb structure features of different types of sweet breads (commercial and added with Chia flour) and their relation with fractal dimension, as a way to propose simple procedures to quantify structural changes that could have an effect on bread quality.

Materials and Methods

Commercial Bread Samples

Two sets of experiments were carried out, one to determine the best resolution for scanning and the thresholding method to apply and the other to analyze the suitability of the method to quantify the crumb features and their relation with fractal dimension of texture for different types of sweet breads. For these experiments, different kinds of sweet bread were chosen. Danish bread for the selection of the resolution settings and three other kinds of commercial sweet breads (Fig. 2) for the evaluation of crumb bread structure: Danish bread (*cuerno*), yeasted sweet bread (*concha*) and pound cake (*panqué*). These breads were selected based on its crumb heterogeneity that would allow a wider range of particle sizes. Eight samples of each kind of these breads were used in the study and all samples were bought at a local bakery in Mexico City.

Sweet Bread Samples Added with Chia Flour

As a way to have more samples with different crumb structure, besides of analyzing the effect of adding Chia (*Salvia hispanica*) flour at different levels on bread quality, sweet yeasted breads were prepared. The bread making process was carried out as reported by Tlapale-Valdivia et

al. (2010) by mixing until optimum dough development 6.9 g of instant active dry yeast (Nevada oro; Safmex), 60 g of sugar (Great Value; Walmart), 3.6 g of salt (La Fina; Sales del Itsmo), 36 g of skim milk powder (Svelty Nestle), 61.5 g of fresh egg (Bachoco), 48 g of shortening (bizcocho saborex; Natural de Alimentos) and 18 or 36 g of Chia flour (*S. hispanica* L, 2009 harvest, Hidalgo, Mexico; 21.2 ± 0.2 g protein/100 g sample (db), 6.0 ± 0.08 g ash/100 g sample (db), 36.7 ± 0.6 g fat/100 g sample (db)), mixed with 282 or 264 g of wheat flour, respectively (alveographic deformation energy of 300×10^{-4} J; 11.56 g protein/100 g sample(db)) and the quantity of water required to reach the flours water absorption as obtained from the farinographic analysis. Mixing was carried out in the farinograph mixing bowl unit (Brabender OHG, Duisburg, Germany). The fermentation process was divided into three bulk fermentation steps (80, 40 and 25 min) and one proofing step (55 min) at constant temperature (32 °C) and humidity (85%). After the final fermentation step, 60 g of dough were weighed, rounded by hand again, placed on a tray and pressure was applied to flatten the samples. Each sample was covered with a dough circular topping (20 g, 3 mm thickness, 8 cm diameter) prepared by mixing sugar (100 g), shortening (100 g) and flour (100 g) and once the product was covered, the topping was marked (“concha” cutter) to obtain a shell pattern. Then, the dough was placed again into the fermentation chamber for 55 min (Precision Scientific Co., USA). Dough samples were baked at 180 °C for 20 min in a rotary oven (Henry Simon Limited, Cheshire, UK). These samples were evaluated by measuring the bread specific volume (method 10–05; American Association of Cereal Chemists, 2000) and crumb colour (Rosales-Juárez et al. 2008). Loaf specific volume was evaluated 120 min after baking using the rapeseed displacement method, while loaf weight was measured immediately after baking. Colour was determined as reported by López-Guel et al. (2010) using a colorimetre (CR-400 Chroma metre, Konica Minolta, USA) with a D65 illumination source at a 0° viewing angle. CIE lab parameters (L^* , $+a^*$, $+b^*$) were obtained.

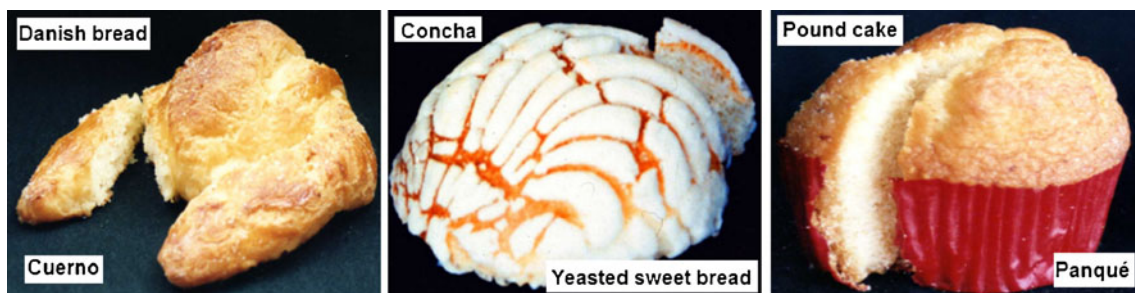


Fig. 2 Different types of commercial sweet bread

Scanning Resolution Setting

Samples of Danish breads were cut in halves using an electric knife (Moulinex Classic 012, France). Sweet bread images were acquired at nine different resolutions (75, 100, 150, 200, 300, 355, 435, 515, 555 dpi) with a flat-bed scanner (Benq Corporation, 5000 Colour Scanner, USA, 1200 optical resolution). During this experiment scanner brightness and contrast parameters (MiraScan6, Benq, Taipei, Taiwan) were kept constant in the default value (zero) (Rosales-Juárez et al. 2008). Images were saved as bitmap files, and sRGB colour. Images were cropped at a field of view (FOV) of 4 × 4 cm that represents approximately 36.5% of crumb bread area; then, images were changed to greyscale (8 bit) using the ImageJ software (National Institutes Health, Bethesda, Md, USA). Segmentation was carried out using the same software by applying the manual thresholding tool, where the grey level threshold was selected by finding each of the peaks of the histogram of frequencies and then the valleys between them, looking for the minimum point of this dip and adjusting manually (Crowley et al. 2000; Gonzales-Barron and Butler 2006). The threshold intensity used for greyscale polarization into binary images was from 110 to 170. The Otsu algorithm was also used (Gonzales-Barron and Butler 2006) for this purpose. The Otsu’s threshold algorithm searches for the threshold that minimizes the intra-class variance, while the manual method locates the threshold by finding each of the peaks of the histogram of frequencies and then the valleys between them (Gonzales-Barron and Butler 2006; On-line docs ImageJ software). The mathematical form of the Otsu’s algorithm has been published elsewhere (Gonzales-Barron and Butler 2006), where the optimal threshold value (t^*), expressed in terms of class probabilities(ω_i) and class means (μ_i) can be obtained by a step sequence: (1) computing the probabilities of each intensity grey level (p_i), (2) setting up the initial probabilities (ω_i) and means (μ_i), (3) stepping through all possible thresholds ($t = 1 \dots$ maximum intensity) and (4) updating ω_i and μ_i to obtain the desired threshold (t^*) which corresponds to the maximum between-class variance (Eq. 1).

$$\sigma_B^2(t) = \frac{[\mu_T \omega(t) - \mu(t)]^2}{\omega(t)[1 - \omega(t)]} \quad (1)$$

Where:

$$\omega(t) = \sum_{i=0}^t p(i) \quad \text{Class probability at the threshold value}$$

$$\mu(t) = \sum_{i=0}^t i p(i) \quad \text{Mean of the class at the threshold value}$$

$$\mu_T = \sum_{i=0}^{L-1} i p(i) \quad \text{Total mean of the whole image}$$

Crumb grain measurements were carried out using the SigmaScan Pro Image Analysis 5.0 software (Jandel Scientific Inc. USA). Two crumb grain features were extracted: cell area, in pixels (A), and the number of cells (objects).

Crumb Bread Structure Evaluation

Two samples per day of each kind of commercial sweet bread were bought during different days, 1 h after taken them out from the oven. They were allowed to cool for at least 2 h at room temperature (20 °C). After cooling, samples were kept inside polyethylene hermetic bags to avoid moisture loss until they were analyzed for crumb structure, which was performed 24 h after baking. Breads were cut in halves with an electric knife (Moulinex Classic 012, France), and these samples were scanned at the resolution value selected from the previous experiment (scanning resolution setting experiment). Images were saved as bitmap format (bmp), in sRGB colour. The same procedure was followed for the sweet bread added with Chia flour.

Pre-Processing of Images

Images were cropped to different FOV depending on the kind of bread, as each type had different form and size, and the only way of obtaining approximately the same proportion of the crumb bread (36–40%) was by selecting different FOVs. This value was selected after measuring the whole bread crumb area of samples, and calculating, as a percentage of the crumb area, the maximum crop that was possible to obtain in the smallest breads. This value was applied during the cropping step for all the samples. Danish bread samples were cropped to 4 × 4 cm, yeasted sweet

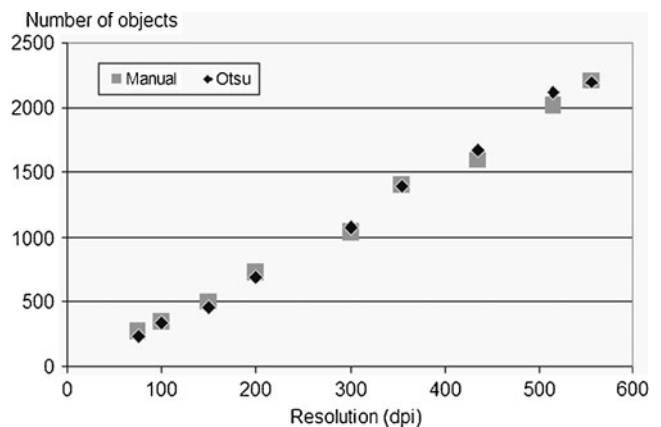
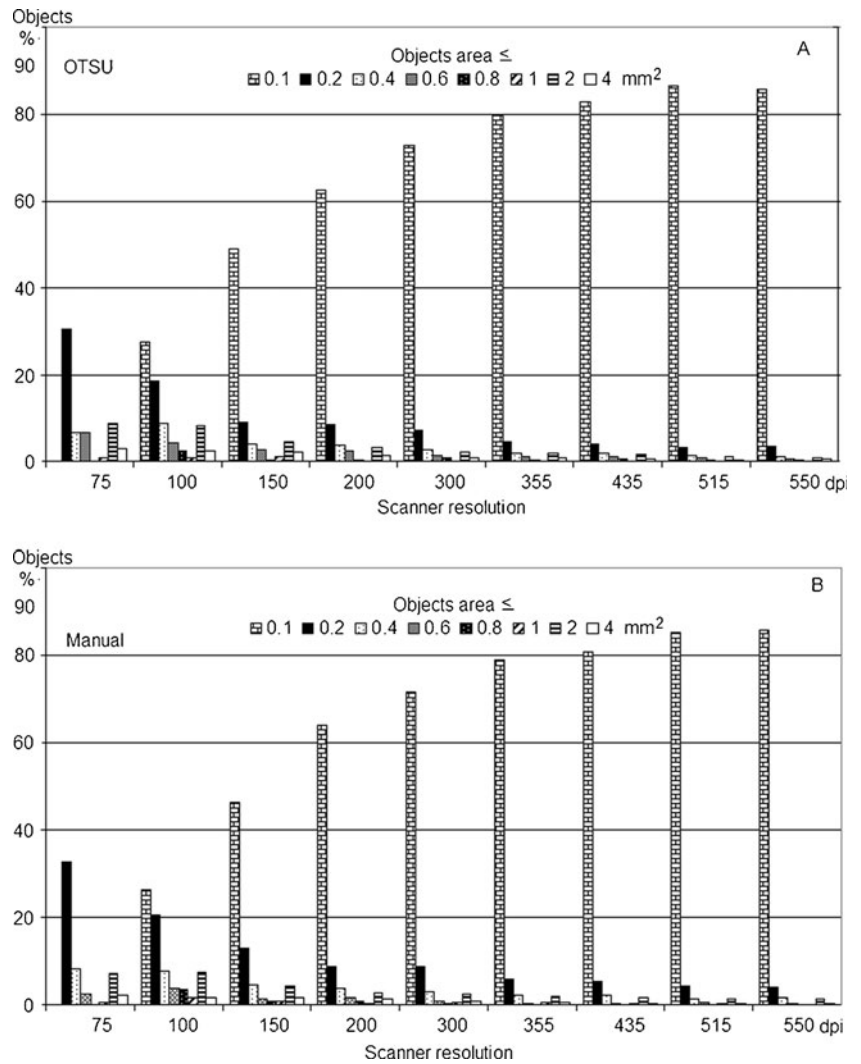


Fig. 3 Effect of varying the scanner resolution on the number of detected objects in sweet bread crumb images, by applying two different thresholding methods (Otsu and Manual)

Fig. 4 Effect of scanner resolution and thresholding methods on the percentage of crumb cells for different area of cells



dough bread to 5.5 × 2.5 cm, pound cake to 4 × 4.1 cm and Chia bread to 3 × 4 cm. All images were thresholded using the Otsu and the manual thresholding tools of the ImageJ Software, where this tools automatically (Otsu) or interactively (Manual) set lower and upper threshold values (110–170), segmenting the image into features of interest and background.

Crumb grain measurements were determined by SigmaScan Pro Image Analysis 5.0 Program. Four crumb grain features were extracted: cell perimeter in pixels (P), cell area, in pixels (A), number of cells (objects), and shape factor (SF) which is a measure of an object’s circularity, where a perfect circle has a SF of 1.0 and a line has a SF approaching to zero. This last parameter is defined as:

$$SF = \frac{4\pi A}{P^2} \tag{2}$$

where SF is the shape factor, A is the cell area and P is the cell perimeter. The fractal dimension of texture was also evaluated.

Fractal Dimension of Texture

The fractal texture of images was evaluated by power law scaling using the Shifting Differential Box Counting

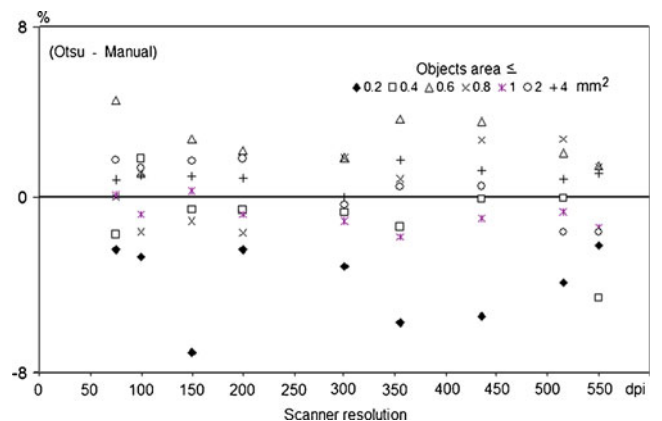


Fig. 5 Difference between Otsu and Manual thresholding methods for the detection of objects with areas larger than 0.1 mm² and smaller equal to 4 mm² as a function of scanner resolution

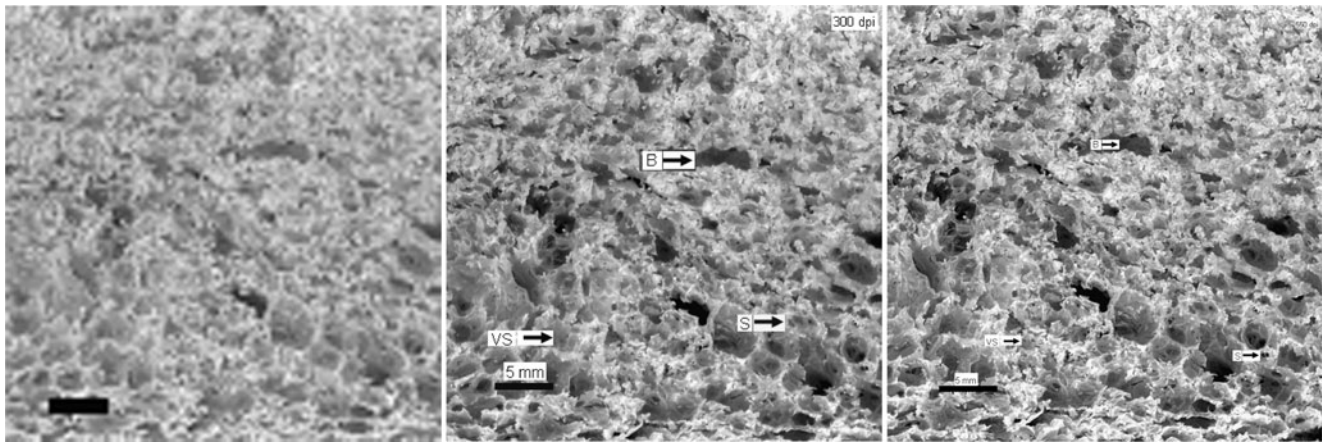


Fig. 6 Crops of bread crumb images acquired at three different resolutions. B: big, S: small, VS: very small pores

method (FD_{SDBC}) which corresponds to the 2-D grey level crumb images as proposed by Wen-Shiung et al. (2003). FD_{SDBC} was calculated using the ImageJ Software by means of the Mapfractalcount plug-in, v 1.0, as shown in Eq. 3, where “ N ” is the number of boxes and “ r ” is the length of the side of box.

$$FD_{SDBC} = \frac{\log(N)}{\log\left(\frac{1}{r}\right)} \quad (3)$$

High values of FD_{SDBC} mean more complex or rougher grey level crumb images, while low values of FD_{SDBC} can be associated to simpler or smoother images.

All measured parameters were analyzed using electronic spreadsheet software (Excel 2000, Microsoft Office Corporation, USA), and where necessary frequency charts (histograms) were obtained grouping results based on crumb cells’ areas, using the histogram function from the analysis data tool of Excel software.

Analysis of Results

Data were analyzed using SigmaStat 3.5 for Windows (Systat Software, Inc. USA), using ANOVA and the Holm–Sidak method or Tukey test as obtained from the software. $P < 0.05$ was considered to be significant. Correlations were obtained by Table Curve2D v5.01 for Windows (Systat software Inc).

Results and Discussion

Figure 3 shows the effect of varying the scanner resolution on the number of counted objects for the two different thresholding methods applied (Otsu and Manual), where no statistical difference ($P < 0.05$) was found between both methods. It is also observed that as resolution increased the number of detected objects also increased, without reaching a steady value; however, when analyzing all data, it was

observed that the number of the smallest objects increased more than the largest ones at higher resolution values. This is presented in Fig. 4 where a frequency analysis was performed by grouping the percentages of objects by their sizes. This evaluation showed that the increasing amount of objects observed as function of resolution was the result of a better segmentation of the smallest particles in the evaluated images as the objects with areas smaller than 0.1 mm^2 significantly increased ($P < 0.05$) their proportion (25–87%) as scanner resolution increased, while the rest of the objects, with larger areas, remained almost invariable (<30%) for both thresholding methods.

In order to have a clearer picture on the potential of both thresholding methods to detect the number of objects when varying the scanning resolution, a new chart was constructed taking into account only the objects with areas

Table 1 Cell density for different kind of sweet breads

Objects with areas (mm^2)		Danish (cells/ cm^2)	Yeastd (cells/ cm^2)	Pound cake (cells/ cm^2)
All	Otsu	170 ± 4.6 ^a	157 ± 4.2 ^d	244.0 ± 3.9 ^f
	Manual	165 ± 6.7 ^a	154 ± 4.6 ^d	246.0 ± 2.5 ^f
$A \geq 0.1$	Otsu	21.0 ± 1.6 ^b	15.8 ± 1.3 ^e	24.1 ± 0.8 ^b
	Manual	21.1 ± 1.8 ^b	15.9 ± 1.4 ^e	27.7 ± 0.4 ^g
$0.1 \leq A \leq 4$	Otsu	19.3 ± 1.5 ^b	14.4 ± 1.2 ^e	22.4 ± 0.9 ^b
	Manual	19.7 ± 1.8 ^b	14.7 ± 1.3 ^e	26.6 ± 0.5 ^g
$0.004 \leq A \leq 4$	Otsu	77 ± 3.5 ^e	72 ± 4.2 ^c	107 ± 2.8 ^h
	Manual	75 ± 4.2 ^e	69 ± 5.6 ^c	112 ± 2.2 ^h

Each result is the average of at least eight repetitions ± standard deviation. Values followed by the same letter are not significantly different (ANOVA and Holm–Sidak or Tukey test). The significance level was 0.05. Cell density was calculated dividing the number of objects of each class (cells) by the area corresponding to the field of view

A mean cell area (mm^2)

Table 2 Mean cell areas for different kinds of sweet breads

Objects with areas (mm ²)		Commercial breads		
		Danish (mm ²)	Yeastd (mm ²)	Pound cake (mm ²)
All	Otsu	0.24 ± 0.02 ^a	0.26 ± 0.04 ^a	0.17 ± 0.02 ^{gfa}
	Manual	0.22 ± 0.02 ^a	0.24 ± 0.05 ^a	0.14 ± 0.006 ^{gff}
$A > 0.1$	Otsu	1.92 ± 0.16 ^b	2.46 ± 0.13 ^d	1.67 ± 0.09 ^{hb}
	Manual	1.71 ± 0.16 ^b	2.19 ± 0.14 ^d	1.16 ± 0.03 ⁱ
$0.1 < A < 4$	Otsu	0.81 ± 0.02 ^c	0.72 ± 0.02 ^c	0.84 ± 0.02 ^c
	Manual	0.83 ± 0.02 ^c	0.7 ± 0.03 ^c	0.84 ± 0.01 ^c
$0.004 < A < 4$	Otsu	0.19 ± 0.03 ^a	0.14 ± 0.01 ^f	0.17 ± 0.02 ^{gfa}
	Manual	0.20 ± 0.03 ^a	0.15 ± 0.01 ^f	0.19 ± 0.02 ^{gfa}

Each result is the average of at least 8 repetitions ± standard deviation. Values followed by the same letter are not significantly different (ANOVA and Holm–Sidak or Tukey test). The significance level was 0.05

A mean cell area (mm²)

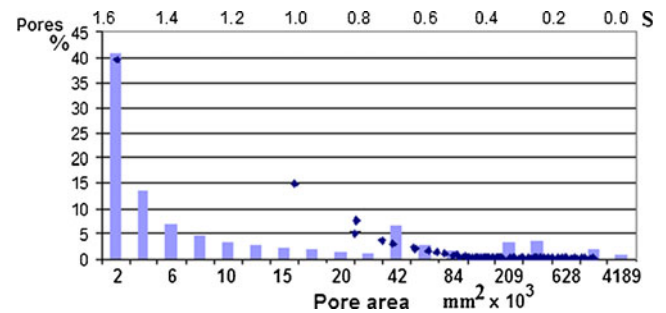
equal or larger than 0.1 mm² and smaller than 4 mm². This selection was based on the sweet bread coarser crumb structure as compare to salty bread, as well as on the fact that the minimum distance between objects to be distinguished by human vision is 0.2 mm, where particles with diameters smaller than this size, might have not been considered as crumb cells, when evaluating crumb structure by bakers experience. On the other hand, Sapirstein et al. (1994) reported that objects with areas larger than 4 mm² could be considered as bread crumb defects. For clarity, data were grouped in seven categories based on the area of objects and plotted as the difference between the percentages of objects detected by the Otsu method minus the percentage of objects detected by the manual method as shown in Fig. 5.

Table 3 Shape factor for different kind of sweet breads

Objects		Danish	Yeastd	Pound cake
All	Otsu	1.0 ± 0.025 ^a	1.03 ± 0.02 ^a	1.05 ± 0.02 ^a
	Manual	1.0 ± 0.032 ^a	1.04 ± 0.03 ^a	1.04 ± 0.02 ^a
$A > 0.1$	Otsu	0.26 ± 0.01 ^b	0.25 ± 0.004 ^b	0.23 ± 0.004 ^b
	Manual	0.26 ± 0.01 ^b	0.25 ± 0.004 ^b	0.25 ± 0.002 ^b
$0.1 < A < 4$	Otsu	0.27 ± 0.01 ^b	0.26 ± 0.004 ^b	0.24 ± 0.003 ^b
	Manual	0.28 ± 0.01 ^b	0.26 ± 0.003 ^b	0.26 ± 0.002 ^b
$0.004 < A < 4$	Otsu	0.572 ± 0.01 ^c	0.59 ± 0.02 ^c	0.58 ± 0.02 ^c
	Manual	0.565 ± 0.01 ^c	0.58 ± 0.02 ^c	0.57 ± 0.02 ^c

Each result is the average of at least 8 repetitions ± standard deviation. Values followed by the same letter are not significantly different (ANOVA and Holm–Sidak or Tukey test). The significance level was 0.05

A mean cell area (mm²)

**Fig. 7** Frequency chart for shape factor (S , black dots) and cell area (bars) of yeastd sweet bread

From the above results, it is possible to observe that the difference between both thresholding methods is less than 8% units and that this value decreased as the cell size increased, which makes both segmentation processes suitable for image analysis for this kind of bread. Gonzales-Barron and Butler (2006) reported the Otsu method produced binary images with high degree of uniformity.

Figure 6 shows the images of bread crumb acquired at three different resolutions; as expected, it was found that the higher resolution setting the best defined images. It can

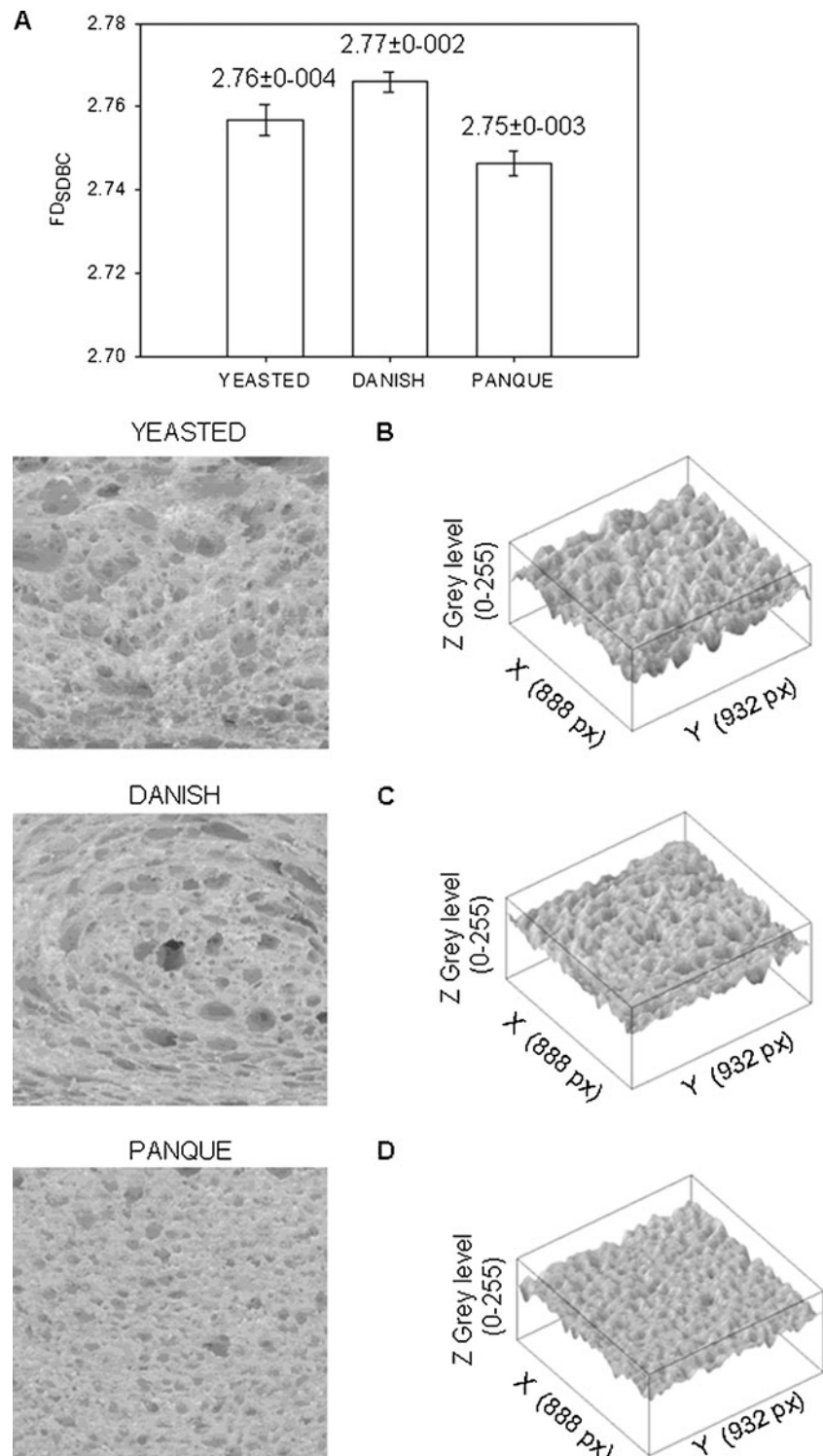
Table 4 Crumb structure of yeastd sweet breads added with “Chia” flour

Objects with areas (mm ²)	Chia flour (g chia flour/100 g flour)		
	0%	6%	12%
Cell Density (Pores/cm²)			
All	178 ± 12 ^a	184 ± 22 ^a	236 ± 22.1 ^b
$A > 0.1$	26 ± 2.7 ^a	25 ± 2.8 ^a	39.7 ± 4.8 ^b
$0.1 < A < 4$	25 ± 2.6 ^a	24 ± 2.2 ^a	38.4 ± 4.0 ^b
$0.004 < A < 4$	103 ± 6.0 ^a	87 ± 13 ^b	158 ± 18.2 ^c
Mean cell area (mm²)			
All	0.24 ± 0.04 ^a	0.26 ± 0.02 ^a	0.15 ± 0.02 ^b
$A > 0.1$	1.78 ± 0.16 ^a	1.57 ± 0.3 ^a	0.82 ± 0.08 ^b
$0.1 < A < 4$	0.67 ± 0.03 ^a	0.58 ± 0.04 ^a	0.56 ± 0.04 ^a
$0.004 < A < 4$	0.16 ± 0.01 ^a	0.14 ± 0.02 ^a	0.16 ± 0.02 ^a
Shape factor			
All	0.97 ± 0.02 ^a	1.0 ± 0.02 ^a	0.93 ± 0.04 ^b
$A > 0.1$	0.31 ± 0.03 ^a	0.31 ± 0.04 ^a	0.37 ± 0.02 ^a
$0.1 < A < 4$	0.31 ± 0.02 ^a	0.32 ± 0.04 ^a	0.38 ± 0.02 ^b
$0.004 < A < 4$	0.64 ± 0.02 ^a	0.59 ± 0.01 ^b	0.70 ± 0.02 ^c

Each result is the average of at least eight repetitions ± standard deviation. Images were thresholded using the Otsu algorithm. Values followed by the same letter in the same row are not significantly different (ANOVA and Holm–Sidak or Tukey test). The significance level was 0.05. Cell density was calculated dividing the number of objects of each class (cells) by the area corresponding to the field of view

A mean cell area (mm²)

Fig. 8 Fractal dimension of texture of the three different kinds of breads. **A** FDSDBC: fractal dimension obtained by means of shifting differential box counting method; **B–D** Dough/crumb images corresponding to surface intensity plot



also be seen from images that crumb is formed by structures of very different sizes, ranging their diameters from <1 to ≥ 4 mm. Considering that particles with diameters smaller than 0.2 mm are too small to be distinguished by human vision, then particles with diameters smaller than this size may have not been considered as crumb cells when evaluating, by eye, crumb structure by

bakers. On the other hand, visual computer assistance methods can detect very small particles, depending on the detection range of the software used to obtain results (Esteller et al. 2006). When applying microscopic techniques, the number of cells has been reported to be even larger than when using traditional image acquisition systems (Gonzales-Barron and Butler 2008c). Under these

circumstances, the selection of the range of particles to be considered to evaluate crumb structure may significantly modify the results.

Table 1 shows cell density results for different kind of commercial sweet breads evaluated by the two different thresholding methods and classified by different cell areas. Cell density was calculated dividing the number of cells (objects) by the FOV.

Data showed that both thresholding methods resulted in similar cell densities, with the exception of pound cake, in which the manual segmentation process produced slightly larger values of cell density, being significantly different ($P < 0.05$) only when considering particles with areas larger than 0.1 mm^2 . Differences among bread crumb structures were also detected, showing that pound cake bread had the largest number of cells per unit area as compared to the other samples. This difference may be a consequence of the bread making process and the ingredients used, such as fat, sugar, additives or others (Kocer et al. 2007). Results were also affected by the range of cell sizes considered in the evaluation. As expected, the largest value was obtained when all the detected objects were used to calculate cell density. These results highlight the importance of establishing and reporting the range of objects sizes to be measured when applying image analysis methodologies.

Table 2 shows that the three kinds of sweet commercial breads presented different cells areas depending on the range of objects used to evaluated them. When all cells were considered, there were not significant differences ($P > 0.05$) in the mean cell areas of Danish and yeasted sweet bread samples, while in all other cases, there were significant variations. Cell areas varied at least ten times between the smallest and the largest value. The kind of thresholding method applied (Otsu and Manual) did not render significant difference ($P > 0.05$) among them.

Table 3 shows the SF for the different commercial breads tested. It can be observed that the form of cells, based on the evaluation of SF, is similar among samples but results depend on the range of cell sizes selected for the evaluation. Both thresholding methods gave similar results.

When analyzing frequency charts of the cell size for different kinds of breads, results showed that smaller cells presented the largest shape factors. It was also observed that as cell size increased, shape factor decreased, which means, as in the other cases, that the value of shape factor depends on the range size used for the evaluation. This information is observed for yeasted sweet bread in Fig. 7.

The crumb features of the yeasted sweet bread added with different concentrations of Chia flour were also analyzed finding that both thresholding methods rendered similar results ($P > 0.05$), and reporting in this work only those obtained when applying the Otsu algorithm (Table 4).

The addition of Chia flour at 6% did not affect cell density, as compared to the non added samples, while the addition of 12% of this flour, increased this parameter. When analyzing the mean cell area of the pores for both Chia flour added breads, it was observed (Table 4) that breads prepared with 12% of Chia flour presented smaller pore areas when all pores or those larger than 0.1 mm^2 were considered in the evaluation. For the other areas' size ranges, the calculations did not render significant differences ($P > 0.05$). These results indicated that the addition of Chia flour could have affected the capacity of dough to entrap air during mixing, resulting in a larger number of air nuclei, which developed into small pores during fermentation and baking. However, these results were not related to the dough mixing behaviour as not significant differences ($P > 0.05$) between farinographic properties of Chia flour samples were observed (data no shown). It is known that Chia seed produces a polysaccharide gel when interacting with water (Bushway et al. 1981; Lin et al. 1994), which could be acting in a similar way as cereal oats, barley or rye β -glucans (Polaki et al. 2010; Lazaridou and Biliaderis 2007), which have been reported to be involved in the development of smaller and more uniform crumb bread pores, by stabilizing the air cells in the dough and preventing their coalescence (Polaki et al. 2010; Wang et al. 1998). On the other hand, the addition of Chia flour promoted a decrement in the specific volume of the breads, resulting in smaller breads as the concentration of Chia was increased, varying from $5.3 \pm 0.1 \text{ g/cm}^3$ (control) to $4.7 \pm 0.1 \text{ g/cm}^3$ (12% addition) and also increasing all the farinographic parameters as compared to the control sample. This effect on farinographic properties could be related to the Chia water absorption capacity, as the fibre fraction of the seed can absorb up to 11.7 g of water per gram of fibre (Vázquez-Ovando et al. 2009), as well as to an increment in the viscosity of the dough promoted by the mucilage presence. Crumb colour was also affected by Chia addition, decreasing the white appearance of the product (72.8 ± 1.3 – 61.7 ± 0.8), and increasing the red and yellow colour as the concentration of Chia was increased in the formulation.

Figure 8, shows the fractal texture (FD_{SDBC}) values for the three kinds of breads tested; different crumb structure

Table 5 Correlation coefficients between cell density and FD_{SDBC} for different areas of cells

Area of objects (mm^2)	Correlation: cell density – FD_{SDBC}
>0.1	0.999
0.1–4.0	0.999
0.004–4	0.923
All objects	0.921

were found, having pound cake the smallest values of FD_{SDBC} as compared to the other breads which indicates that pound cake has the least complex and smoothest crumb texture.

The number of analyzed objects per unit of area correlated well with fractal dimension of texture (Table 5) achieving better correlation coefficients when objects with areas smaller than 0.1 mm^2 or larger than 4 mm^2 were not considered. Fractal dimension could be a suitable indicator of amount of cells generated during processing.

Conclusions

Image analysis was a useful tool to evaluate sweet bread crumb structure, detecting differences among the different kinds of breads analyzed. The thresholding methods applied (Otsu and Manual) rendered similar results; the largest difference between them was no more than 8%. The use of larger resolution values resulted only in an increment of the smallest objects. Crumb structure features results were influenced by the number of detected objects considered in the evaluation, making necessary the establishment of a range of cell sizes to avoid including noise or crumb defects that could make data unreliable. The addition of Chia flour at the highest level seems to be involved in the generation of smaller and more uniform crumb bread pores, maybe by stabilizing the air cells and preventing their coalescence.

References

- Baiano, A., Romaniello, R., Lamacchia, C., & La Notte, E. (2009). Physical and mechanical properties of bread loaves produced by incorporation of two types of toasted durum wheat flour. *Journal of Food Engineering*, *95*, 199–207.
- Barletta, B. J., & Barbosa, C. G. V. (1993). Fractal analysis to characterize ruggedness changes in tapped agglomerated food powders. *Journal of Food Science*, *58*, 1030–1035.
- Barret, A. H., & Peleg, M. (1995). Applications of fractal analysis to food structure. *LWT Food Science and Technology*, *28*, 553–563.
- Bushway, A. A., Belyea, P. R., & Bushway, R. J. (1981). Chia seed as a source of oil polysaccharide and protein. *Journal of Food Science*, *46*, 1349–1350.
- Calderón-Domínguez, G., Chanona-Pérez, J., Ramos-Cruz, A. L., López-Lara, A. I., Tlapale-Valdivia, A. D., & Gutiérrez-López, G. F. (2008). Fractal and image analysis of Mexican sweet bread bubble distribution; influence of fermentation and mixing time. In G. M. Campbell, M. Scanlon, L. Pyle, & K. Niranjan (Eds.), *Bubbles in food 2: Novelty, health and luxury* (pp. 73–81). St. Paul: American Association of Cereal Chemists.
- Chanona, P. J. J., Alamilla, B. L., Farrera, R. R. R., Quevedo, R., Aguilera, J. M., & Gutiérrez, L. G. F. (2003). Description of the convective air drying of a food model by means of the fractal theory. *Food Science and Technology International*, *9*(3), 207–213.
- Chevallier S, Zúñiga R & Le-Bail A (2010) Assessment of bread dough expansion during fermentation. *Food Bioprocess Technology*, doi:10.1007/s11947-009-0319-3.
- Collar, C., Bollain, C., & Angioloni, A. (2005). Significance of microbial transglutaminase on the sensory mechanical and crumb grain pattern of enzyme supplemented fresh pan breads. *Journal of Food Engineering*, *70*, 479–488.
- Crowley, P., Grau, H., & Arendt, E. K. (2000). Influence of additives and mixing time on crumb grain characteristics of wheat bread. *Cereal Chemistry*, *77*(3), 370–375.
- Datta, A. K., Sahin, S., Sumnu, G., & Keskin, S. O. (2007). Porous media characterization of breads baked using novel heating methods. *Journal of Food Engineering*, *79*, 106–116.
- Esteller, M. S., & Lannes, S. (2008). Production and characterization of sponge-dough bread using scalded rye. *Journal of Texture Studies*, *39*, 56–67.
- Esteller, M. S., Zancanaro, O., Jr., Santos-Palmeira, C. N., & Lannes, S. C. S. (2006). The effect of kefir addition on microstructure parameters and physical properties of porous white bread. *European Food Research and Technology*, *222*, 26–31.
- Gonzales-Barron, U., & Butler, F. (2006). A comparison of seven thresholding techniques with the k-means clustering algorithm for measurement of bread-crumbs features by digital image analysis. *Journal of Food Engineering*, *74*(2), 268–278.
- Gonzales-Barron, U., & Butler, F. (2008a). Fractal texture analysis of bread crumb digital images. *European Food Research and Technology*, *226*, 721–729.
- Gonzales-Barron, U., & Butler, F. (2008b). Prediction of panellists' perception of bread crumb appearance using fractal and visual textural features. *European Food Research and Technology*, *226*, 779–785.
- Gonzales-Barron, U., & Butler, F. (2008c). Crumb features quantification by cryo-scanning electron microscopy images. In G. M. Campbell, M. Scanlon, L. Pyle, & K. Niranjan (Eds.), *Bubbles in food 2: Novelty, health and luxury* (pp. 89–97). St. Paul: American Association of Cereal Chemists.
- Hatcher, D. W., Symons, S. J., & Manivannan, U. (2004). Developments in the use of image analysis for the assessment of oriental noodle appearance and colour. *Journal of Food Engineering*, *61*, 109–117.
- Hernández, B., Cuevas, N. L., Shama-Levy, M. E. A., Ramírez, S. C. I., García, F. R., Rivera, J. A., et al. (2003). Factores asociados con sobrepeso y obesidad en niños mexicanos en edad escolar. Resultados de la encuesta urbana de alimentación y nutrición de la zona metropolitana de la Ciudad de México. *Salud Pública México*, *45*(4), 558–564.
- Kerdpiroon, S., & Devahastin, S. (2007). Fractal characterization of some physical properties of a food product under various drying conditions. *Drying Technology*, *25*(1), 135–146.
- Kocer, D., Hicsasmaz, Z., Bayindirli, A., & Katnas, S. (2007). Bubble and pore formation of the high ratio cake formulation with polydextrose as a sugar and fat replacer. *Journal of Food Engineering*, *78*, 953–964.
- Lagrain, B., Boeckx, L., Wilderjans, E., Delcour, J. A., & Lauriks, W. (2006). Non-contact ultrasound characterization of bread crumb: application of the Biot-Allard model. *Food Research International*, *39*, 1067–1075.
- Lagrain, B., Leman, P., Goesaert, H., & Delcour, J. A. (2008). Impact of thermostable amylases during bread making on wheat bread crumb structure and texture. *Food Research International*, *41*, 819–827.
- Lassoued, N., Babin, P., Della Valle, G., Devaux, M. F., & Réguerre, A. L. (2007). Granulometry of bread crumb grain: considerations of 2D and 3D image analysis at different scale. *Food Research International*, *40*, 1087–1097.

- Lazaridou, A., & Biliaderis, C. G. (2007). Molecular aspects of cereal β -glucan functionality: physical properties, technological applications and physiological effects. *Journal of Cereal Science*, *46*, 101–118.
- Lin, K. Y., Daniel, J. R., & Whistler, R. L. (1994). Structure of chia seed polysaccharide exudate. *Carbohydrate Polymers*, *23*, 13–18.
- López-Guel EC, Lozano-Bautista F, Mora-Escobedo R, Farrera-Rebollo RR, Chanona-Pérez J, Gutiérrez-López GF, Calderón-Domínguez G (2010) Effect of soybean 7 S protein fractions, obtained from germinated and nongerminated seeds, on dough rheological properties and bread quality. *Food Bioprocess Technology*, doi:10.1007/s11947-009-0277-9.
- Pedreschi, F., Aguilera, J. M., & Brown, C. (2000). Characterization of food surfaces using scale-sensitive fractal analysis. *Journal of Food Processing Engineering*, *23*, 127–143.
- Peleg, M., & Normand, M. D. (1985). Characterization of the ruggedness of instant coffee particles by natural fractals. *Journal of Food Science*, *50*(3), 829–831.
- Pérez-Nieto, A., Chanona-Pérez, J. J., Farrera-Rebollo, R. R., Gutiérrez-López, G., Alamilla-Beltrán, L., & Calderón-Domínguez, G. (2010). Image analysis of structural changes in dough during baking. *LWT Food Science and Technology*, *43*, 535–543.
- Polaki, A., Xasapis, P., Fasseas, C., Yanniotis, S., & Mandala, I. (2010). Fiber and hydrocolloid content affect the microstructural and sensory characteristics of fresh and frozen stored bread. *Journal of Food Engineering*, *97*, 1–7.
- Pyler, E. J. (1988). *Baking science and technology* (pp. 740–775). Kansas: Sosland.
- Rahman, M. S. (1997). Physical meaning and interpretation of fractal dimensions of fine particles measured by different methods. *Journal of Food Engineering*, *32*, 447–456.
- Ribotta, P. D., Pérez, G. T., Añón, M. C., & León, A. E. (2010). Optimization of additive combination for improved soy-wheat bread quality. *Food and Bioprocess Technology*, *3*, 395–405.
- Riva, M., & Liviero, S. (2000). Image analysis approach to characterize the bread cooking kinetic. *Industria Alimentare*, *39* (395), 593–660.
- Rogers, D. E., Day, D. D., & Olewnik, M. C. (1995). Development of an objective crumb grain measurements. *Cereal Foods World*, *40*, 498–501.
- Rosales-Juárez, M., González-Mendoza, B., López-Guel, E. C., Lozano-Bautista, F., Chanona-Pérez, J. J., Gutiérrez-López, G., et al. (2008). Changes on dough rheological characteristics and bread quality as a result of the addition of germinated and non-germinated soybean flour. *Food and Bioprocess Technology*, *2* (1), 152–160.
- Rosell, M. C., & Santos, E. (2010). Impact of fibers on physical characteristics of fresh and staled bake of bread. *Journal of Food Engineering*, *98*, 273–281.
- Sapirstein, H. D., Roller, R., & Bushuk, W. (1994). Instrumental measurement of bread crumb grain by digital image analysis. *Cereal Chemistry*, *71*(4), 383–391.
- Scanlon, M. G., & Aghal, M. C. (2001). Bread properties and crumb structure. *Food Research International*, *34*, 841–864.
- Skendi, A., Biliaderis, C. G., Papageorgiou, M., & Izydorczyk, M. S. (2010). Effects of two barley β -glucan isolates on wheat flour dough and bread properties. *Food Chemistry*, *119*, 1159–1167.
- Takano, H., Naito, S., Ishida, N., Koizumi, K., & Kano, H. (2002). Fermentation process and grain structure of baked breads from frozen doughs. *Journal of Food Science*, *67*(2), 2725–2733.
- Theiler, J. (1990). Estimating fractal dimension. *Journal of the Optical Society of America A*, *7*(6), 1055–1073.
- Tlapale-Valdivia, A. D., Chanona-Pérez, J. J., Mora-Escobedo, R., Farrera-Rebollo, R. R., Gutiérrez-López, G. F., & Calderón-Domínguez, G. (2010). Dough and crumb grain changes during mixing and fermentation and their relation with extension properties and bread quality of yeasted sweet dough. *International Journal of Food Science & Technology*, *45*(3), 530–539.
- Vázquez-Ovando, A., Rosado-Rubio, G., Chel-Guerrero, L., & Betancur-Ancona, D. (2009). Physicochemical properties of a fibrous fraction from chia (*Salvia hispanica* L.). *LWT Food Science and Technology*, *42*(1), 168–173.
- Wang, L., Miller, R. A., & Hoseney, R. C. (1998). Effects of (1–3)(1–4) β -D-glucans of wheat flour on breadmaking. *Cereal Chemistry*, *75*, 629–633.
- Wen-Shiung, C., Shang-Yuan, Y., & Chih-Ming, H. (2003). Two algorithms to estimate fractal dimension of gray-level images. *Optical Engineering*, *42*(8), 2452–2464.
- Zayas, I. Y. (1993). Digital image texture analysis for bread crumb grain evaluation. *Cereal Foods World*, *38*(10), 760–766.